Chapter 12

THE FRAGMENTARY RIGHT MAXILLA OF THE SCLADINA I-4A JUVENILE

Christine VERNA & Michel TOUSSAINT

Michel Toussaint & Dominique Bonjean (eds.), 2014.
The Scladina I-4A Juvenile Neandertal (Andenne, Belgium), Palaeoanthropology and Context
Études et Recherches Archéologiques de l'Université de Liège, 134: 223-232.

1. Introduction

After the initial discovery of the right hemi-mandible Scla 4A-1, in July 1993, sorting of the faunal collections found previously at Scladina in the same stratigraphic unit was undertaken. During this laboratory work, which mainly took place in the second part of 1993, several human teeth and a right partial maxilla were identified. The teeth had been discovered a few years earlier, from 1990 until 1992, and the maxilla in February 1992, but none of these fossils had been recognized as human and more specifically as Neandertal at that time. The partial maxilla comes from Square D30 and was first attributed to former Layer 4A; however, according to the recent and more precise analysis of the stratigraphy of the cave (Chapter 3), it would seem to originate from Unit 4A-POC, even if an origin from the top of Unit 4A-CHE cannot be entirely ruled out (Chapter 5).

Below we provide a description of the partial maxilla and compare its morphology to samples of subadult Neandertals as well as Early Modern Humans associated with Middle and Upper Palaeolithic industries. Each individual is attributed to a dental development stage based on dental eruption as follows: S1: deciduous dentition only; S2: deciduous dentition and M1 fully erupted; S3: mixed dentition with the M1 and at least another fully erupted permanent tooth (but usually not the M2); S4: permanent dentition only, with the M2 fully erupted, but not the M3. The Scladina Child belongs to the S3 stage.

Maxillas, in particular immature ones, are fragile skeletal elements and are therefore relatively scarce in the fossil record. In addition, individuals from age class S1 are far more abundant than those from the other age classes, which considerably limits our comparison of Scladina to children of similar age. Our Neandertal samples include nine individuals distributed as follows: four from dental stage S1 (Engis 2, Roc de Marsal, Subalyuk 2, Devil's Tower), two S2 individuals (La Quina 18; Krapina 46), three S3 (Kůlna, Krapina 47, Teshik-Tash) and two S4 (Krapina 48, 49). The Pleistocene Modern Human sample includes the Middle Palaeolithic individuals Qafzeh 4, Qafzeh 11 and Mugharet-el-Aliya as well as eight individuals associated with Upper Palaeolithic industries (UPMH). Five of these belong to the S1 age class (Le Figuier, Grotte des Enfants 1 and 2, La Madeleine, Le Placard 31); one to S2 (Saint-Germain-la-Rivière 7); one to either the S2 or S3 age classes (Le Placard 33) and one to S4 (Cova del Parpalló). All data were gathered from the study of the original specimen except for Teshik-Tash and Cova del Parpalló for which the data were recorded from casts.

2. State of preservation

The Scla 4A-2 maxilla is a single fragment from the right mid-facial region that retains part of the alveolar and palatine processes and a small part of the body (Figure 1). The fragment is 50 mm in length and 25 mm in both height and width. The bone is broken along a subhorizontal section at the level of the floor of the nasal fossa, so that the frontal process, the upper part of the body and the zygomatic process are all missing. A small part of the nasal floor is preserved and, laterally, parts of the floor of the maxillary sinus are revealed by the breakage.

Medially, the bone is preserved up to the sagittal midline in its lower part and retains the interdental wall between the permanent maxillary incisor sockets as well as a portion of the contact surface with the left maxilla (Figures 1e & 3a). However, the breakage runs laterally upwards so that the inferior margin of the piriform aperture is missing except for a very small portion at the level of the interalveolar septum between the two central incisors.

The fragment extends laterally from the midline to the mesial part of both the distobuccal

Figure 1: Scla 4A-2 right maxilla at 1:1 scale. (a) external (antero-lateral), (b) internal, (c) superior, (d) inferior, (e) medial and (f) posterior views. Photographs Joël Éloy, AWEM.

and lingual roots of the M^1. The alveoli of the right incisors, canine and dm1 are well preserved, with their medial side almost intact whereas the lateral one is eroded (I^1, I^2) or largely destroyed (C, dm^1). Only a small part of the palatine process is preserved. It extends backward for about 30 mm from the *orale* and does not reach the transverse suture.

Six right teeth, found isolated in former Layer 4 (see Chapter 5 for more details about the stratigraphic origin of the fossils), can be refitted in the maxilla (see Chapter 13): both permanent incisors (Scla 4A-11 & 14), the permanent canine (Scla 4A-16), both deciduous molars (Scla 4A-7 & 5), and the first permanent molar (Scla 4A-4). In addition, the unerupted Scla 4A-2/P^4 is visible in the bottom of the dm^2 socket. The second maxillary molar (Scla 4A-3) and the third molar germ (Scla 4A-8) have also been found.

3. Morphology

3.1. Antero-lateral view: external face of the body

Anteriorly, the very small preserved portion of the inferior margin of the piriform aperture, above the I^1-I^2 interdental septum (ca. 6.5 mm long), shows two crests separated by a prenasal groove (*fossa intranasalis*). In addition, the presence of a *fossa intranasalis* suggests a pattern similar to the Franciscus (2003) nasal margin category 5 (spinal crest fused to the lateral one and partially fused to the turbinal) or 6 (partial fusion of the spinal and turbinal crests). We shall recall here that 67% of Neandertals show configuration 5 (n = 21), whereas only 3% of Upper Palaeolithic Modern Humans and none of the specimens from Qafzeh and Skhul (Franciscus, 2003) present this pattern. Note also that configuration 6 is very rare and was never observed in these Pleistocene samples. Group differences are even more marked when only subadult individuals are considered (see Table 1).

Based on the preserved portion of the nasoalveolar clivus, the subnasal height (M48-1, Martin, 1928) would be higher than 18 mm and may be estimated at close to 19.5 mm. This value is higher than all Neandertals belonging to age class S1 (Table 2; Figure 2a) but very close to Engis 2 (19.3 mm). It falls well within the range of the class 3 Neandertals, being higher than Teshik-Tash but lower than Kůlna and Krapina 47, and is much lower than the older Krapina 49 individual. When compared to Pleistocene Modern Humans the subnasal height of Scladina is higher than Qafzeh 10 (age class S2) and above all Upper Palaeolithic individuals from all age classes, falling well outside their range of variation (m = 12.5;

sd = 1.4; m+2sd = 15.3). Finally, the value measured on Scla 4A-2 is also well above the mean obtained by Minugh-Purvis (1993) for samples of modern humans of similar ages (mid- and late-childhood, m = 14.8 and 14.5 respectively) and at the upper limit of the variation of a sample of 10-12 dental development ages (range = 11-19, m = 14.9, n = 7). Therefore, the subnasal height of Scladina is rather high and consistent with the range of variation of Neandertals, who have a high nasoalveolar region when compared to recent humans (Maureille, 1994). Although Minugh-Purvis (1988) suggested that this high subnasal height seen in adult Neandertals would not develop before late childhood, our data (Table 2) as well as other studies (e.g. Madre-Dupouy, 1992; Krovitz, 2003) show that young Neandertals (age class S1) already have a higher subnasal height than Upper Palaeolithic and modern children of similar ages. This might not be the case when compared to earlier modern humans (associated with Middle Palaeolithic or Middle Stone Age industries) but insufficient data are available in the fossil record.

The nasoalveolar clivus is a rather flat surface, only slightly superio-inferiorly concave, and marked by the *jugum* of the two incisors. Laterally, the vertical canine *jugum* is visible, although partially destroyed. Behind it, above the molar sockets, the body takes a quite strong lateral orientation upwards. Although not enough is preserved to assess the infra-orbital topography, this lateral projection of the body above the post-canine dental alveoli makes it unlikely that this piece could have exhibited any strong *incurvatio inframalaris sagittalis* or *incurvatio horizontalis* as described in the 'flexion' type infraorbital surface of Sergi (1948). Furthermore, the preserved morphology shows that the root of the zygomatic process, i.e. the zygomaticoalveolar crest, emerges at the level of m^2/M^1, at a location more posterior than Subalyuk 2 and La Quina 18, similar to the younger individual Roc-de-Marsal, but more anterior than all the other S2-S3 individuals (Table 1). The emergence of the crest is overall slightly more anterior in the UPMH sample (Table 1), being most often located at the m^2 in the

	Specimen	Age class	Internal nasal floor pattern	Nasal margin configuration	Zygoalveolar crest placement
	Scladina	**S3**	**bilevel**	**5/6?**	**m2M1**
	Devil's Tower[1] (Gibraltar)	S1	bilevel	–	–
	Engis 2 (Belgium)	S1	bilevel	5	–
	Roc de Marsal 1 (France)	S1	bilevel	5	m2M1
NEAND	Subalyuk 2 (Hungary)	S1	bilevel	5	m1m2
	La Quina 18 (France)	S2	bilevel	5	m1m2l/m2r
	Krapina 46 (Croatia)	S2	–	–	M1
	Kůlna (Czech Republic)	S3	–	5	M1
	Krapina 47 (Croatia)	S3	sloped	3	M1
	Teshik-Tash[c] (Uzbekistan)	S3	–		M1
	Krapina 48 (Croatia)	S4	level	–	–
	Krapina 49 (Croatia)	S4	sloped	2	–
	Qafzeh 4 (Israel)	S2	–	4	M1
MPMH	Qafzeh 11[1] (Israel)	S2	level	4	
	Mugharet-el-Aliya[1,2] (Morocco)	S3	sloped	3/7	
	Arene Candide 6[1] (Italy)	S1	bilevel	3,7	
	Lagar Velho[1] (Portugal)	S1	sloped/bilevel?	7	
	Le Figuier (France)	S1	level	3	m2
	Grotte des Enfants 1 (Italy)	S1	level	1	m2
	Grotte des Enfants 2 (Italy)	S1	level	1	m2
UPMH	La Madeleine (France)	S1	((level	3	
	Le Placard 31 (France)	S1	level	–	m2M1
	Saint-Germain-la-Rivière 7 (France)	S2	–	–	m2M1
	Le Placard 33 (France)	S2/3	level	–	m2M1
	Cova del Parpalló[c] (Spain)	S4	level	1	M1

Table 1: Morphological features. Internasal floor pattern and nasal margin configuration following the categories defined by Franciscus (2003). **NEAND**: Neandertals; **MPMH**: Middle Palaeolithic Modern Humans; **UPMH**: Upper Palaeolithic Modern Humans. Otherwise indicated, all data were recorded by the authors on the original specimens. [c] data collected on a cast; [1] data from Franciscus, 2003; [2] data from Minugh-Purvis, 1993. See the text for the definition of the age classes.

	Taxon	Age Class	Subnasal Height	LA1	LA2	LP1	LP2
Scladina I-4A	**NEAN**	**S3**	**19.5**	**12.7**	**17.1**	**22.7**	**17.2**
Dederiyeh 2[(1)]	**NEAN**	S1	16.4				
Engis 2	**NEAN**	S1	19.3	12.1	18.7		
Roc de Marsal	**NEAN**	S1	15.0	14.0	20.8	18.0	17.6
Subalyuk 2	**NEAN**	S1	15.9	9.7	16.8	23.6	18.0
Kůlna	**NEAN**	S3	24.8	10.9	16.17		13.3
La Quina 18 L	**NEAN**	S2				21.6	16.6
Krapina 47 L	**NEAN**	S3	22.9	15.5	20.6		
Teshik-Tash[(c)]	**NEAN**	S3	18.3	15.3	21.0	22.1	15.3
Krapina 49 L	**NEAN**	S4	27.4	16.6	20.7		
Qafzeh 4 R	**MPMH**	S2				20.1	15.0
Qafzeh 10[(2)]	**MPMH**	S2	18.6				
Arene Candide 5B[(3)]	**UPMH**	S1	14.6				
Arene Candide 11[(3)]	**UPMH**	S1	13.4				
Le Figuier L	**UPMH**	S1	11.4	11.3	17.1	21.4	16.6
Grotte des Enfants 2	**UPMH**	S1	11.3	10.5	16.0		15.6
Grotte des Enfants 1	**UPMH**	S1	11.4	10.5	15.5		
La Madeleine	**UPMH**	S1	13.6	10.6	15.7	21.5	
Le Placard 61401-31 R	**UPMH**	S1		11.8	17.7		
Le Placard 61401-33 R	**UPMH**	S2/S3		13.6	19.3		15.2
Saint-Germain-Rivière 7 R	**UPMH**	S2				20.2	15.6
Sungir 4[(4)]	**UPMH**	S3	11.0				
Cova del Parpalló 1[(c)]	**UPMH**	S4	13.5	13.6	18.2	17.2	11.9

Table 2: Subnasal height and arcade length measurements. **NEAND**: Neandertals; **MPMH**: Middle Palaeolithic Modern Humans; **UPMH**: Upper Palaeolithic Modern Humans. Otherwise indicated, all data were recorded by the authors on the original specimens. [(c)] data collected on a cast; [(1)] data from Dodo et al., 2002; Ishida & Kondo, 2002; [(2)] data from Tillier, 2002; [(3)] data from Henry-Gambier, 2001; [(4)] data from Minugh-Purvis, 1993. See the text for the definition of the age classes.

S1 age class, m^2/M^1 in the S2/S3 classes, reaching the M^1 only in the single individual belonging to age class S4. According to Minugh-Purvis (1993), the root of the zygomatic process emerges at the level of m^2/M^1 in 56% of 9 modern children aged 7 to 8 years, and above the M^1 in 44% of them. However, it emerges at or posterior to the M^1 in 100% of the individuals over 8 years of age. It has been shown that in adult Neandertals the root of the zygomatic process emerges more posteriorly relative to the dentition than in recent humans (Rak, 1986; Trinkaus, 1987; Maureille, 1994). Indeed, the zygomaticoalveolar crest emerges at the level of M^2 or M^2/M^3 on all but one adult Neandertals (n = 9, Verna, 2006), whereas it is anterior to the M^2 on 90% of the recent humans (n = 159; Maureille, 1994). This posterior placement of the zygomaticoalveolar crest has been linked to the mid-facial prognathism and topography characterizing Neandertals (Rak, 1986; Trinkaus, 1987). It has also been suggested that allometric relationships between infraorbital surface topography and infraorbital size could explain the Neandertal infraorbital surface topography (Maddux & Franciscus, 2009), although not entirely (Freidline et al., 2012). The Scladina pattern appears rather anterior when compared to similarly aged Neandertals, which might then reflect a rather low mid-facial prognathism and/or a relationship with size factors (i.e. an infraorbital region not as large as other Neandertals). Not enough of the mid-facial region is however preserved to test this hypothesis.

3.2. Superior view: floors of nasal fossa and maxillary sinus

As stated above, an anterior portion of the nasal floor (ca. 28 mm in length and 16 mm in width) is preserved. Medially, a very small part of the incisive crest is visible at the level of the incisive canal opening as well as tiny parts of the nasal crest behind that opening. Below that opening, in medial view, the incisive canal runs down vertically and emerges on the palatine process (see

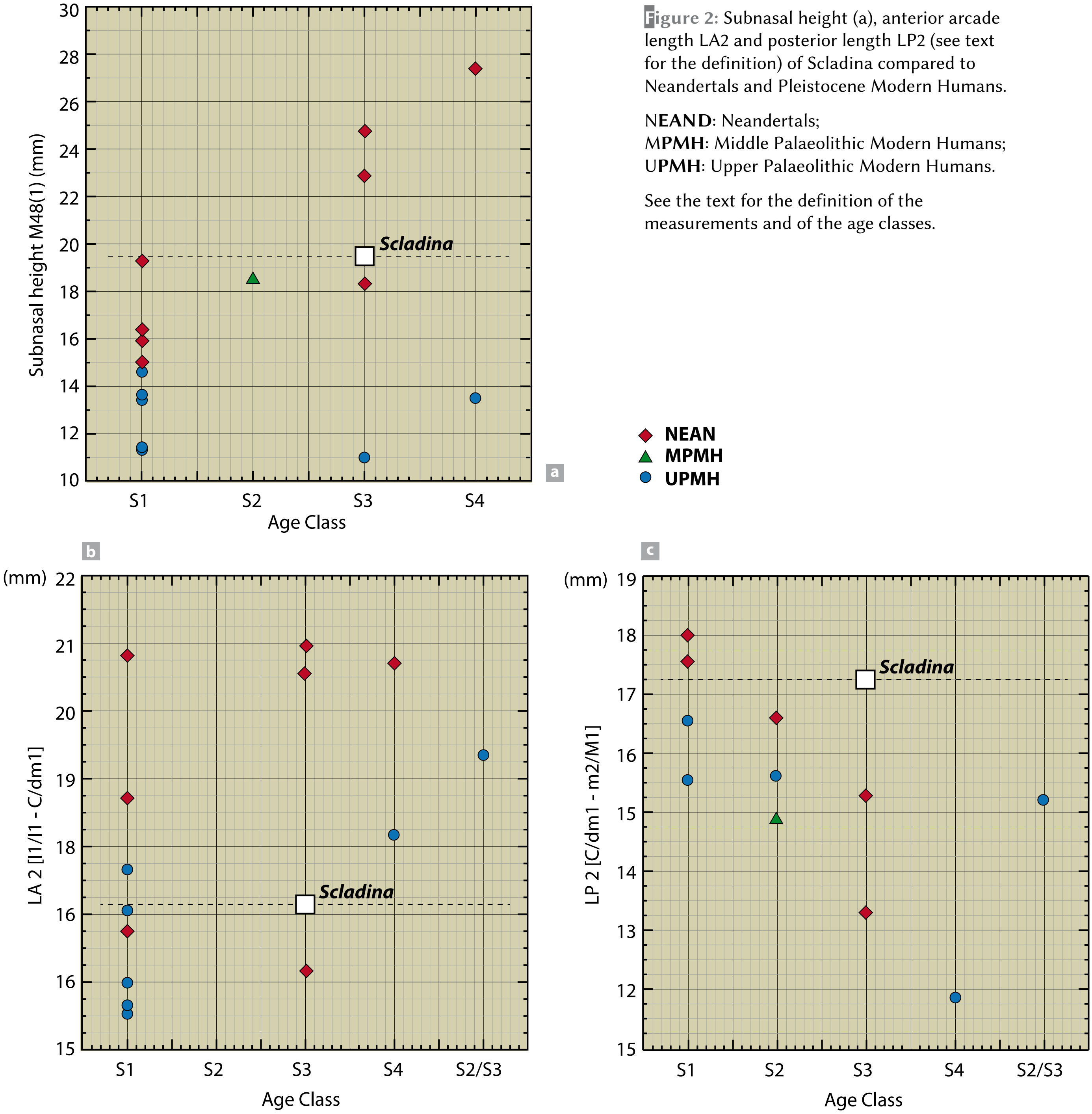

Figure 2: Subnasal height (a), anterior arcade length LA2 and posterior length LP2 (see text for the definition) of Scladina compared to Neandertals and Pleistocene Modern Humans.

NEAND: Neandertals;
MPMH: Middle Palaeolithic Modern Humans;
UPMH: Upper Palaeolithic Modern Humans.

See the text for the definition of the measurements and of the age classes.

below). Postero-laterally, on the preserved portion of the floor of the maxillary sinus, two small holes (ca. 3 mm) reveal the two root apices of the still imbedded P^4 (Figure 3a).

Despite the absence of the nasal spine region, the preserved morphology allows us to assess the internal configuration of the nasal floor, following the criteria of Franciscus (2003). The Scladina nasal floor shows a bilevel configuration, a pattern also shown by five out of eight subadult Neandertals (S2-S4) but only one or two UPMH (Table 1). According to Franciscus's (2003) data, this bilevel pattern is also found in 87% of adult Neandertals (n = 15) but only one of seven MPMH (Near East and North Africa) and none of the adult UPMH (n = 30).

Furthermore, we can observe the premaxillary suture (*sutura premaxillaris*; see Maureille & Braga, 2002) in the anterior part of the nasal floor (Figures 3a & 4). The suture runs medio-laterally across the entire portion of the nasal floor that is preserved, following a rectilinear path.

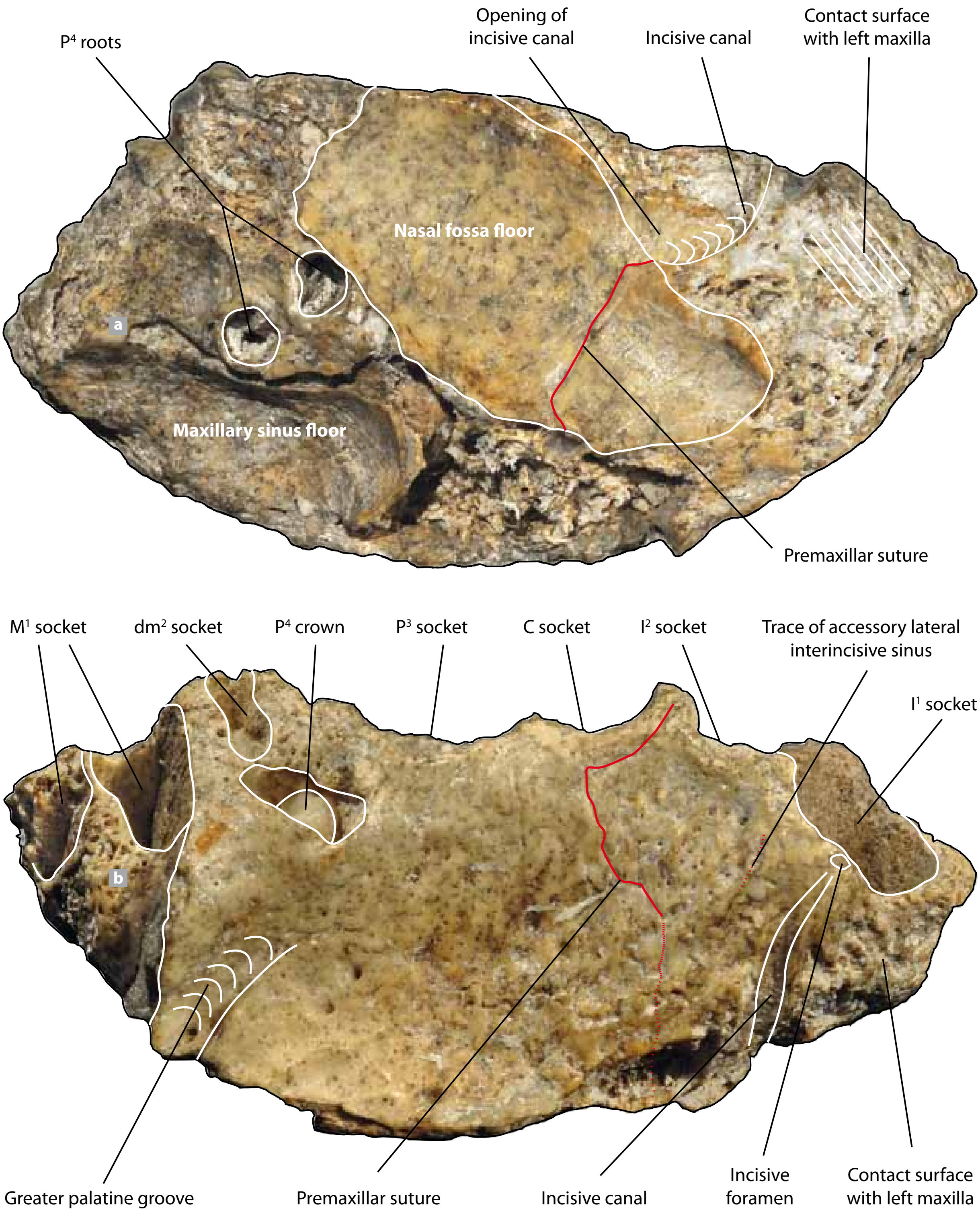

Figure 3: Superior (a) and inferior (b) views of the Scladina maxilla with main anatomical details underlined (photographs Joël Éloy, graphics Sylviane Lambermont, AWEM).

3.3. Inferior view: alveolar and palatine process

The palatine process is insufficiently preserved to allow any of the standard measurements of the palatal and dental arch. In order to compare the dental arch size of Scladina to that of other Upper Pleistocene individuals we took several linear measurements of the arcade length. We measured these on the inner side of the alveolar process and

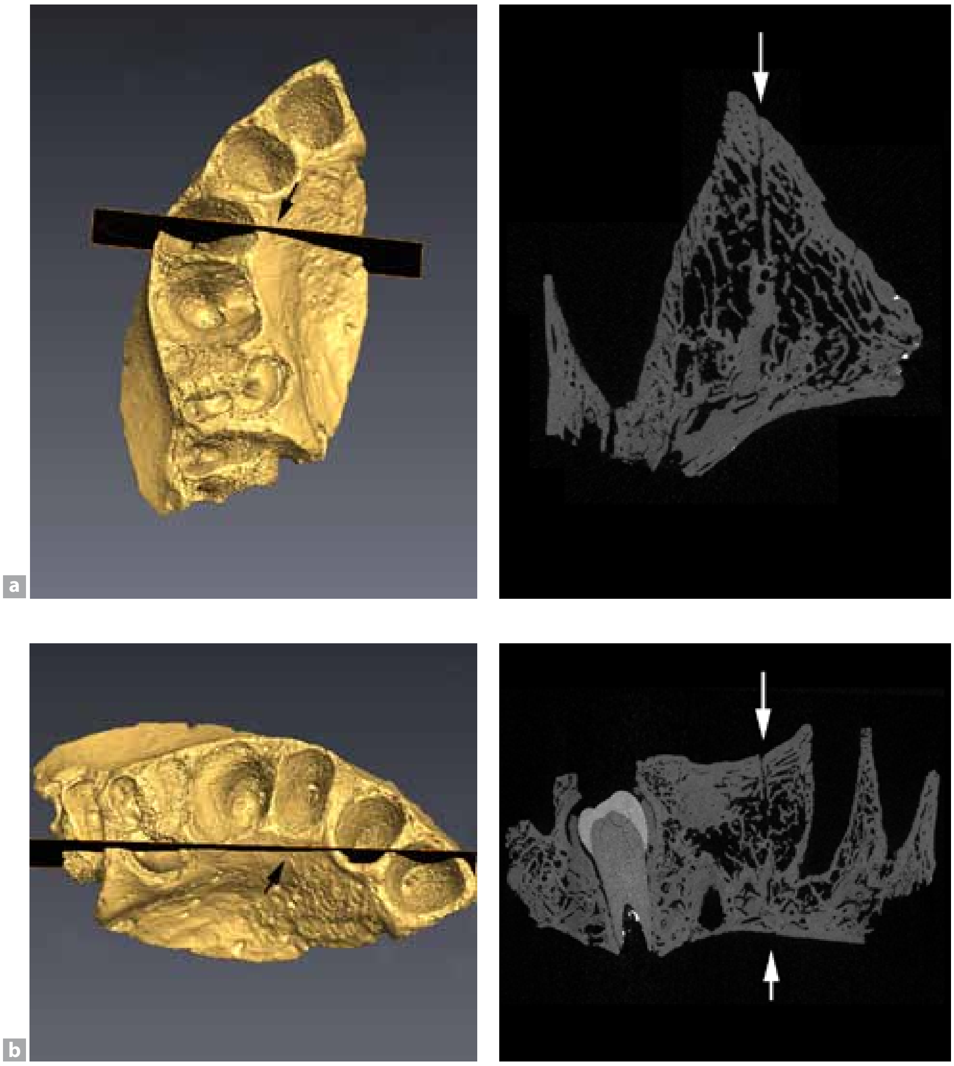

Figure 4: micro-CT scans data showing the premaxillary suture (as indicated by the arrows).

the landmarks selected were the lowest and most medial points on the interalveolar septum. Two lengths (LA 1 and LA2) provide an estimate of the anterior length of the arcade: LA1 = distance I^1/I^1 (or i^1/i^1) to I^2/C (or i^2/dc); LA2 = distance I^1/I^1 (or i^1/i^1) to C/P^3 (or dc/dm^1). In addition, two measurements were taken for the posterior part of the arcade: LP1 = distance I^2/C (or i^2/dc) - m^2/M^1 (P^4/M^1); LP2 = distance C/P^3 (c/m^1) - m^2/M^1 (P^4/M^1).

The distance from the midline (I^1/I^1) to the I^2/C septum of Scladina (LA1 = 17.1 mm) falls well within the range of variation of both Neandertal and UPMH samples, even though it is rather high when compared to the UPMH and rather small when compared to other Neandertals (Table 2). Indeed, it falls within the range of variation of the younger S1 Neandertals (with I^1 and I^2 not yet erupted), and close to Engis 2. Although it is higher than Kůlna, it falls well below other S3 and S4 individuals (Krapina 47, 49 and Teshik-Tash). The same distance to the P^3-dm^1 septum (LA2) is also rather low, falling in the lower part of the Neandertal range (all age classes pooled) and well within the UPMH range (Table 2 & Figure 2b). The distance I^2/C – m^2/M^1 (LP1) is by contrast among the highest values of our comparative samples, being higher than all Neandertals but one (Subalyuk 2), Qafzeh 4 (MPMH) and above all UPMH individuals (Table 2). The same is true when only the first two cheek teeth are considered, i.e. the distance LP2 between C/P^3 (or c/dm^1) and P^4/M^1 (or dm^2/M^1). Overall, Scladina falls among the highest Neandertal values, above Qafzeh 4 and above all UPMH individuals (Figure 2c).

On the anterior part of the alveolar process, the right wall of a unique incisive foramen can be observed behind the medial wall of the I^1 socket.

		Scla	Ded1	DevTo	Eng2	PAze	RdM	Sub2	LQ18	Kra47	Kůlna	TTash
NEAND	Age class	**S3**	S1	S1	S1	S1	S1	S1	S2	S3	S3	S3
	Origin of the data	**(1)**	(2)	(3)	(1)	(3)	(1)(3)	(1)	(1)	(3)	(1)	(3)
	Premaxillary suture above *crista conchalis*	**x**		x	Yes		Yes	Yes		x	x	
	Premax. suture below *crista conchalis*	**x**		x	Yes		Yes	Yes		x	x	
	Premax. suture on the floor of nasal fossae	**Yes**		No	Yes		Yes	Yes		x	Trace	
	Premax. suture on palatal face	**Yes**	Yes	No	Yes	Yes	Yes	Yes	Yes	No	No	Yes
	Lateral scondary interincisive sinus	**Trace**	Yes	No	Yes	Yes	Yes	Yes	Trace	x	No	
	Medial secondary interincisive sinus	**Trace?**	Yes	No	Yes	Yes	Yes	Yes	x	x	No	

		Qafz4	GE1	GE2	Le Figuier	Plac31	Plac33	StGer7
MPMH & UPMH	Age class	S2	S1	S1	S1	S1	S2/3	S2
	Origin of the data	(1)	(1)	(1)	(1)	(1)	(1)	(1)
	Premaxillary suture above *crista conchalis*	No	Yes	Yes		Yes	x	
	Premax. suture below *crista conchalis*	x		Yes		Yes	x	
	Premax. suture on the floor of nasal fossae	x	(No)	Yes		Yes	Yes	(Yes)
	Premax. suture on palatal face	Trace	Yes	Yes	Yes	Yes	Yes	
	Lateral secondary interincisive sinus	Yes	Yes	Yes	Yes	x	No	
	Medial secondary interincisive sinus	Yes	x	No	No	No	No	

Table 3: Expression of the premaxillary suture in the fossil specimens. **NEAND**: Neandertals; **MPMH:** Middle Palaeolithic Modern Humans; **UPMH:** Upper Palaeolithic Modern Humans. Origin of the data: (1) This Study; (2) Dodo et al., 2002; (3) Maureille & Bar, 1999. See the text for the definition of the age classes. **Scla** = Scladina; **Ded1** = Dederiyeh; **DevTo** = Devil's Tower; **Eng2** = Engis 2; **PAze** = Pech de l'Azé (Patte, 1957); **RdM** = Roc de Marsal; **Sub2** = Subalyuk 2; **LQ18** = La Quina 18; **Kra47** = Krapina 47; **TTash** = Teshik-Tash; **Qafz4** = Qafzeh 4; **GE** = Grotte des Enfants; **Plac** = Le Placard; **StGer7** = Saint-Germain-Rivière 7.

All Neandertals show a unique incisive foramen, whereas among recent humans there is more variation, sometimes with additional openings. A deep, larger palatine groove emerges distally at the level of the dm²/M¹ septum.

The premaxillary suture (*sutura premaxillaris*) can be observed on the palatine process (Figures 3b & Figure 4). It runs first distally from the I²-C interalveolar septum along the canine alveolar edge, and turns then medially and slightly anteriorly. As described above, this suture is also visible on the nasal floor (but its possible presence on the lateral wall of the nasal fossa cannot be confirmed). In addition, slight traces of the secondary interincisive sinus are visible behind the I1-I2 interdental septum. Finally, slight traces close to the incisive canal might reflect the presence of a medial interincisive sinus (see Maureille & Bar, 1999) but the traces are not clear enough to assert it. The premaxillar suture is well observed on the micro-CT data (Figure 4), which show that the suture is not restricted to the surface of the palatal face but runs upwards inside the bone Micro-CT data also show that the lateral interincisive sinus is open in its medial part.

A similar pattern, with an open premaxillary suture on the palatal face as well as on the nasal floor is observed on all the younger Neandertals from the S1 dental development with the exception of Devil's Tower. The suture is also visible on the palatal face of La Quina 18 and Teshik-Tash, but is closed on Krapina 47 and Kůlna (Table 3). The premaxillary suture is also most often visible on the palatal face and nasal floor of the UPMH individuals, showing no difference in expression with Neandertals (but the data set is limited). It has been suggested that the closure of the premaxillary suture is delayed on Neandertals compared to recent humans (Maureille, 1994; Coqueugniot, 1998; Maureille & Bar, 1999; Maureille & Braga, 2002). The premaxillar suture on Scladina is still open on part of its path, adding to the evidence provided by Maureille & Bar (1999) on younger individuals. A delayed closure of the suture might have allowed a longer growth period of the Neandertal midface. In addition, Maureille & Bar (1999) have stressed that the presence of two interincisive sinuses is much more frequent than in recent humans, possibly because of their larger incisor size. Our data suggest that UPMH show most often only one sinus in a pattern similar to recent humans (Table 3). More data are however needed on Pleistocene Early Modern Humans.

4. Conclusions

The maxilla of Scladina is a rather small fragment retaining only parts of the right body, palatine and alveolar processes. Its high subnasal height (estimated) and the bilevel configuration of its internal nasal floor are consistent with the Neandertal group. The location of the zygoalveolar crest is however not as posterior as similarly aged Neandertals. In addition, the anterior part of its dental arcade is rather short when compared to other Neandertals, which is consistent with the rather low cervical area of the anterior teeth (see Chapter 13) which fall in the lower part of the Neandertal range. Finally, the premaxillary suture is visible on the palatal face and on the nasal floor and still open on a large part of its path as shown by the Ct-scan data. This add to previous studies suggesting a delayed closure of the premaxillar suture on Neandertals compared to recent humans.

Acknowledgements

We would like to thank the following people and institutions who provided research access to the original fossil remains included in the comparative samples C. Schwab and M.-S. Larguèze, Musée d'Archéologie nationale, Saint-Germain-en-Laye (France); J.-J. Cleyet-Merle, Musée national de Préhistoire, Les Eyzies-de-Tayac (France); I. Pap, Hungarian Natural History Museum, Budapest (Hungary); K. Valoch, P. Neruda, Anthropos Institute of the Moravian Museum; Prof. H. de Lumley, A. Vialet and S. Renault from the Institut de Paléontologie Humaine (Paris); Ph. Mennecier, A. Fort and L. Huet from the Musée de l'Homme, Paris (France); E. Poty, University of Liège; J. Radovčić, Croatian Natural History Museum (Zagreb).

The authors are also grateful to Sylviane Lambermont and Joël Éloy, graphic artists at the Association wallonne d'Études mégalithiques as well as Jean-François Lemaire, Service de l'Archéologie en province de Liège du Service public de Wallonie, for all the figures. For taking the time to improve the English text, Jean-François Lemaire again and Rebecca Miller, University of Liège.

References

Coqueugniot H., 1998. *Variabilité morphologique de la tête osseuse au cours de l'ontogenèse. L'exemple des enfants de l'espèce* Homo sapiens. Unpublished PhD thesis, Université Bordeaux 1, 334 p.

Dodo Y., Kondo O. & Nara T., 2002. The Skull of the Neanderthal Child of Burial No.1. In T. Akazawa & S. Muhesen (eds.), *Neanderthal Burials: Excavations of the Dederiyeh Cave, Afrin, Syria*. Kyoto, International Research Center for Japanese Studies. Roma, L'Erma di Bretschneider: 93–137.

Franciscus R. G., 2003. Internal nasal floor configuration in *Homo* with special reference to the evolution of Neandertal facial form. *Journal of Human Evolution*, 44: 701–729.

Freidline S. E., Gunz P., Janković I., Harvati K. & Hublin J.-J., 2012. A comprehensive morphometric analysis of the frontal and zygomatic bone of the Zuttiyeh fossil from Israel. *Journal of Human Evolution*, 62: 225–241.

Gower C. G., 1923. A contribution to the morphology of the apertura piriformis. *American Journal of Physical Anthropology*, 6: 27–36.

Henry-Gambier D., 2001. *Les Enfants de Grimaldi (Grotte des Enfants, Site des Baoussé-Roussé, Italie), Anthropologie et Palethnologie Funéraire (avec les contributions de M.-A. Courty, É. Crubézy, B. Kervazo)*. Paris, Éditions du Comité des travaux historiques et scientifiques & Éditions de la Réunion des Musées Nationaux, 14, 177 p.

Ishida H. & Kondo O., 2002. The Skull of the neanderthal Child of Burial No.2. In T. Akazawa & S. Muhesen (eds.), *Neanderthal Burials: Excavations of the Dederiyeh Cave, Afrin, Syria*. Kyoto, International Research Center for Japanese Studies. Roma, L'Erma di Bretschneider: 271–297.

Krovitz G. E., 2003. *Shape and growth differences between Neandertals and modern humans: Grounds for a species-level distinction?* In J. L. Thompson, G. Krovitz & A. J. Nelson (eds.), *Growth and Development in the Genus Homo*. Cambridge University Press: 320–342.

Maddux S. D. & Franciscus R. G., 2009. Allometric scaling of infraorbital surface topography in Homo. *Journal of Human Evolution*, 56: 161–174.

Madre-Dupouy M., 1992. *L'Enfant du Roc de Marsal*. Paris, Éditions du Centre national de la recherche scientifique, Cahiers de Paléoanthropologie, 299 p.

MARTIN R., 1928 (2nd ed.). *Lehrbuch der Anthropologie in systematischer Darstellung*, II, Jena, Fischer, 3 vols.

MAUREILLE B., 1994. *La face chez Homo erectus et Homo sapiens : recherche sur la variabilité morphologique et métrique*. Unpublished PhD thesis, Université de Bordeaux 1, 486 p.

MAUREILLE B. & BAR D., 1999. The premaxilla in Neandertal and early modern children: ontogeny and morphology. *Journal of Human Evolution*, 37: 137–152.

MAUREILLE B. & BRAGA J., 2002. Between the incisive Bone and Premaxilla. From African apes to *Homo sapiens*. In N. MINUGH-PURVIS & K. J. MCNAMARA (eds.), *Human evolution through developmental change*. Baltimore, Johns Hopkins University Press: 464–478.

MINUGH-PURVIS N., 1988. *Patterns of craniofacial growth and development in Upper Pleistocene Hominids*. Unpublished PhD thesis. University of Pennsylvania, 657 p.

MINUGH-PURVIS N., 1993. Reexamination of the Immature Hominid maxilla From Tangier, Morocco. *American Journal of Physical Anthropology*, 92: 449–461.

PATTE E., 1957. *L'enfant néanderthalien du Pech de l'Azé*. Paris, Masson & Cie, 230 p.

SERGI S., 1948. Sulla morfologia della facies anterior corporis maxillae nei paleantropi di Saccopastore e del Monte Circeo. *Rendiconto della Reale Accademia Nazionale dei Lincei,classe de Scienze Fisiche, Matematiche e Naturali, ser. 8:* 387–394.

RAK Y., 1986. The Neanderthal: a new look at an old face. *Journal of Human Evolution,* 15: 151–164.

TILLIER A.-M., 2002. *Les Enfants Moustériens de Qafzeh. Interprétation Phylogénétique et Paléoauxologique*. Paris, Éditions du Centre national de la recherche scientifique, Cahiers de Paléoanthropologie, 239 p.

TRINKAUS E., 1987. The Neandertal face: evolutionary and functional perspectives on a recent hominid face. *Journal of Human Evolution*, 16: 429–443.

VERNA C., 2006. *Les restes humains moustériens de la Station Amont de La Quina – (Charente, France). Contexte archéologique et constitution de l'assemblage. Étude morphologique et métrique des restes crânio-faciaux. Apport à l'étude de la variation néandertalienne*. Unpublished PhD thesis, Université de Bordeaux 1, 629 p.